

## VELOCITY PROFILES FOR THE LAMINAR FLOW OF STRUCTURALLY VISCOUS FLUIDS BETWEEN PARALLEL PLANES

Yu. V. Kostylev, V. I. Popov, and E. M. Khabakhpasheva

Zhurnal Prikladnoi Mekhaniki i Tekhnicheskoi Fiziki, No. 2, pp. 100-103, 1966

**ABSTRACT:** In [1], a rheological equation for structurally viscous fluids was proposed and the expediency of distinguishing a special subclass of fluids with a linear flow law was demonstrated.

The present paper compares the theoretical and experimental velocity profiles of structurally viscous fluids.

The tangential stress distribution for stabilized flow in a flat channel is linear, i. e., it is expressed by

$$\tau = \tau_w \xi, \quad (\xi = y/h) \quad (1)$$

where  $\tau_w$  is the tangential shear stress at the wall,  $y$  is the distance from the channel axis, and  $h$  is the channel half-width.

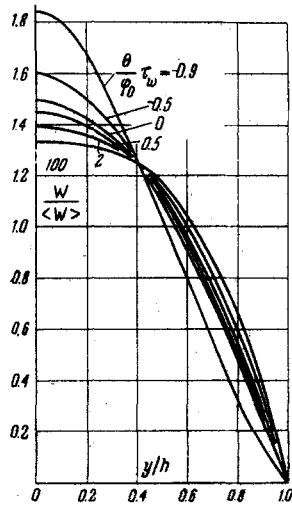


Fig. 1

The velocity profile is defined by the formula

$$W = h \int_{\xi}^1 \varphi(\tau) \tau d\xi, \quad (2)$$

where  $\varphi(\tau)$  is the fluidity of the fluid. For a linear flow law of the form

$$\varphi = \varphi_0 + \theta(\tau - \tau_1), \quad (3)$$

assuming that  $\tau_1 \approx 0$  (where  $\tau_1$  is the limit strength of the fluid structure), we get

$$W = \frac{h\tau_w\varphi_0}{2} \left[ (1 - \xi^2) + \frac{2}{3} \frac{\theta}{\varphi_0} \tau_w (1 - \xi^3) \right], \quad (4)$$

$$\frac{W}{\langle W \rangle} = 1.5 \frac{1 - \xi^2 + \frac{2}{3} \frac{\theta}{\varphi_0} \tau_w (1 - \xi^3)}{1 + 0.75 \frac{\theta \tau_w}{\varphi_0}}, \quad (5)$$

where  $\langle W \rangle$  is the mean flow rate,  $\theta$  is the coefficient of structural stability of the fluid, and  $\varphi_0$  is zero-fluidity of the fluid—i. e., the fluidity as  $\tau \rightarrow 0$ .

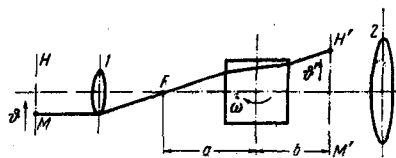


Fig. 2

The velocity profiles calculated from formula (5) for various values of the parameters  $\theta\tau_w/\varphi_0$  are given in Fig. 1.

For fluids whose fluidity increases with stress ( $\theta > 0$ ), the velocity profile is flatter than for ordinary Newtonian fluid flows: fluids for which  $\theta < 0$  exhibit the contrary effect.

The ratio  $\theta\tau_w/\varphi_0$ —which is a measure of the profile variation—shows that the velocity distribution depends on the magnitude of the shear stress.

It should be noted that the exponential relation between the tangential shear stress and velocity gradient usually employed [2-4] leads to the relation

$$\frac{W}{\langle W \rangle} = \frac{1 + 2n}{1 + n} [1 - \xi^{(1+n)/n}] \quad (6)$$

according to which the velocity profile is independent of  $\tau_w$ .

**Procedure for measuring the velocity profile.** The experimental equipment, in the form of a closed circuit, provides a constant rate of flow with the aid of a tank of constant level. Measurements are performed in a rectangular transparent channel, 4.25 by 1.02 cm in size, at a distance of 90 cm from the channel inlet. The velocity profile is measured by a specially designed device based on the principle of optical-mechanical image scanning of small particles moving in the flow. The optical scheme of the device is shown in Fig. 2, where 1) is the lens, 2) is the eyepiece, and 3) is the prism.

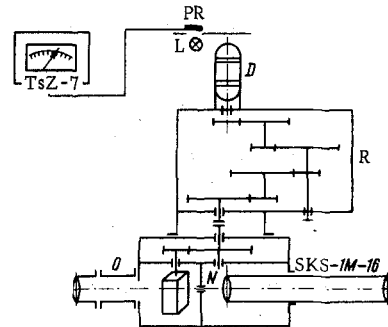


Fig. 3

To the displacement of a particle that moves at velocity  $v$  in the focal plane of the lens MH corresponds the displacement of its image in the focal plane of the eyepiece M'H' at a certain velocity  $v'$  that depends on the angular velocity of prism rotation and on the optical and geometrical characteristics of the system. By varying the rotational velocity of the prism, it is possible to reach a situation in which the image of a particle will appear fixed. The velocity with which a particle moves in the flow and the rotational velocity of the prism are related by the simple relationship  $v = K\omega$ , where  $K$  is the instrument constant, which may be determined by calibration, and  $\omega$  is the angular velocity of prism rotation.

An essential part of the device is a modified SKS-1M-16 high-speed motion picture camera (Fig. 3). The prism is rotated by a dc motor via a two-speed reducer R (in the present test series, the reduction coefficients  $a_0$  and  $a_1$  were equal to 0.24 and 1.27, respectively).

On the shaft of the motor is mounted a disk with 12 holes through which the light from the lamp L falls onto a photoresistor PR. The photoresistor applies pulses to a TsZ-7 frequency meter.

The velocity was calculated from the formula

$$v = Ba_{0,1} \nu$$

where  $B = 0.054$  is the instrument constant determined by calibration from the rotational velocity of the circumference of a disk of given radius,  $a_{0,1}$  are the reduction coefficients, and  $\nu$  is the frequency indicated by the TsZ-7 frequency meter.

A narrow light beam ("knife-edge beam"), incident from above, illuminates the axial plane of the channel. The lens of the device is focused onto the same region, as is its mouthpiece 0 that provides the required magnification, and whose optical axis is perpendicular to the axis of the light beam in the channel. The slot N isolated a 0.26-mm thick layer from the flow. The items observed were the luminous traces of small particles or air bubbles, measuring several microns, which happened to be present in the illuminated region. The device was mounted on a KM-6 cathetometer capable of counting dislocations in the vertical plane with an accuracy of 0.01 mm.

The performance of the device and of the hydrodynamic loop was checked in special tests employing water. For laminar flow of water, the experimental velocity distributions were of the type

$$W / \langle W \rangle = 1.5 (1 - \xi^2), \quad (7)$$

Maximum scatter of the separate points was  $\pm 4\%$ .

**Measurement results.** The curves obtained with a capillary-type viscometer are given in Fig. 4, where curve (a) corresponds to the results obtained with a 4% solution of polyvinyl alcohol in water, the curve (b) corresponds to results obtained with an 0.4% solution of sodium carboxymethyl cellulose in water; it is seen that below a certain value of  $\tau_w$ , the fluidity curve is satisfactorily approximated by formula (3).

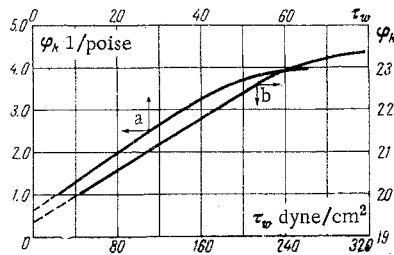


Fig. 4

It should be noted that capillary viscometers do not yield values of apparent fluidity in the region of small tangential shear stresses. The value of  $\varphi_0$  was, therefore, obtained by extrapolation of the flow curve with respect to the y axis.

The tests aimed at determining the velocity distribution of the polyvinyl alcohol solution were performed for  $\theta\tau_w/\varphi_0$  values roughly equal to 2, 4, and 6.

The tangential shear stresses at the channel wall were determined from the corresponding velocity gradients and were checked with the aid of changes in pressure.

The measurement results are given in Fig. 5, where the points 1, 2, and 3 correspond to  $\theta\tau_w/\varphi_0$  values of 2, 4, and 6, respectively, for a 4% solution of polyvinyl alcohol in water. For an 0.4% solution of sodium carboxymethyl cellulose, the value of  $\theta\tau_w/\varphi_0$  was found to be as low as 0.005, even for large Reynolds numbers ( $R \approx 600$ ), because of the high zero-fluidity and small  $\theta$  coefficient of this solution. In conformance with expectations, the velocity distribution obtained in this case practically did not differ from the velocity distribution for laminar flow of ordinary Newtonian fluids (7).

For a channel flow of the polyvinyl alcohol solution, a separation of the velocity profiles as a function of the value of the  $\theta\tau_w/\varphi_0$  complex can be readily observed. For  $\theta\tau_w/\varphi_0 = 6$  ( $\tau_w = 43$  dyne/cm<sup>2</sup>), the

experimental velocity profiles agree with the theoretical ones to within 1.5 to 2%, which is an indication of the accuracy of formula (5) obtained on the basis of a linear flow law for a range of shear stresses encountered in the practice.

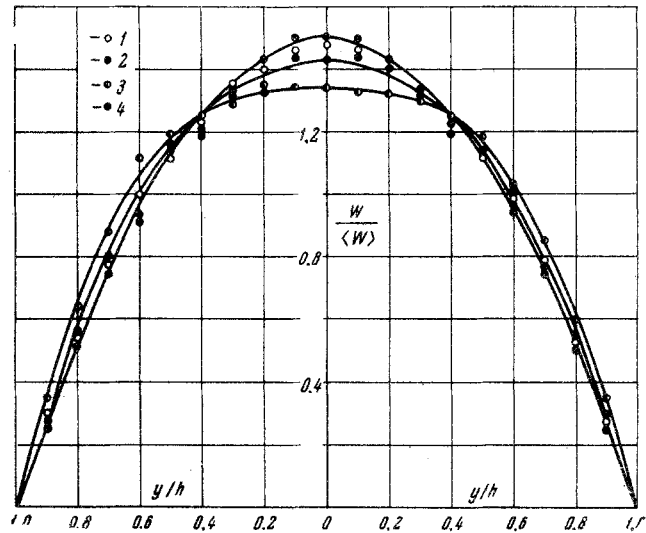


Fig. 5

With decreasing values of the  $\theta\tau_w/\varphi_0$  complex, the discrepancy between the experiment and the data calculated from formula (5) increases, reaching 5% at  $\theta\tau_w/\varphi_0 = 2$ . This may be associated with the inadmissibility of comparing experimental data with formula (5) at very small  $\tau$  values. Indeed, in the derivation of formula (5) it was assumed that the stability limit of the fluid structure  $\tau_1 = 0$ . In reality, however, in the region of very small  $\tau$  values, the fluid may still not exhibit "non-Newtonian" properties, so that the portion of the cross section occupied by a seemingly "Newtonian" flow will increase with decreasing  $\tau_w$ . For large values of  $\tau_w$ , this effect is practically absent. Unfortunately, we still lack sufficiently accurate methods for determining fluidity at very small shear stress values, so that linear extrapolation of the fluidity curve may be considered as justified. Such an extrapolation, however, may lead to a certain discrepancy between theory and experiment in the region of small  $\tau_w$  values.

REFERENCES

1. S. S. Kutateladze, V. I. Popov, and E. M. Khabakhpasheva, "Contribution to the hydrodynamics of variable-viscosity fluids," PMTF, no. 1, 1966.
2. W. K. Wilkinson, Non-Newtonian Fluids [Russian translation], Izd. "Mir," 1964.
3. J. Ulbrecht and P. Mitschka, Chemické inženýrství neneutonských kapalin. Nakladatelství Československé Akademie Věd, Praha, 1965.
4. S. A. Bostandzhiyan and A. M. Stolin, "Flow of non-Newtonian fluids between two parallel planes," Izv. AN USSR, Mekhanika, no. 1, 1965.

14 July 1965

Novosibirsk